Journal of Rare Earths 41 (2023) 1627–1635

Contents lists available at ScienceDirect

Journal of Rare Earths

journal homepage: http://www.journals.elsevier.com/journal-of-rare-earths

Preparation of CeO_2 abrasives by reducing atmosphere-assisted molten salt method for enhancing their chemical mechanical polishing performance on SiO_2 substrates☆

Ning Xu [a, b, *], Jiahui Ma [a, b], Qi Liu [a, b], Yuxin Luo [a, b], Yongping Pu [a, b]

[a] School of Material Science and Engineering, Shaanxi University of Science & Technology, Xi'an, 710021, China
[b] Shaanxi Key Laboratory of Green Preparation and Functionalization for Inorganic Materials, Xi'an, 710021, China

ARTICLE INFO

Article history:
Received 17 May 2022
Received in revised form
13 October 2022
Accepted 21 October 2022
Available online 29 October 2022

Keywords:
CeO_2
Chemical mechanical polishing (CMP)
Reducing atmosphere
Material removal rate (MRR)
Molten salt method
Rare earths

ABSTRACT

Ce^{3+} as the active site on the CeO_2 abrasive surface is the key to enhancing the material removal rate (MRR). The CeO_2 abrasives with high chemical activity were prepared by the molten salt method under a reducing atmosphere. The crystal structure and morphology of CeO_2 abrasives were characterized by X-ray diffraction (XRD), scanning electron microscopy (SEM), transmission electron microscopy (TEM), Fourier transform infrared spectroscopy (FT-IR), ultraviolet–visible diffuse reflectance spectroscopy (UV–Vis DRS), and X-ray photoelectron spectroscopy (XPS). The CeO_2 abrasives were obtained under different atmospheres (Air, Ar, and Ar/H_2). With the enhancement of the reducing atmosphere, the morphology of the abrasives transforms from spherical to octahedral, while more oxygen vacancies and Ce^{3+} are generated on the surface of CeO_2 abrasives. The CMP experiments show that the MRRs of the CeO_2-Air, CeO_2-Ar, and CeO_2-Ar/H_2 abrasives on SiO_2 substrates are 337.60, 578.74, and 691.28 nm/min, respectively. Moreover, as confirmed by atomic force microscopy (AFM), the substrate surfaces exhibit low roughness (~0.5 nm) after being polished using all of the prepared samples. Especially, the MRR of CeO_2-Ar/H_2 abrasives is increased by 104.76% compared with CeO_2-air abrasives. The improved CMP performance is attributed to the increased Ce^{3+} concentration and the octahedral morphology of the abrasives enhancing the chemical reaction and mechanical removal at the abrasive–substrate interface.

1. Introduction

CMP (Chemical Mechanical Polishing)[1] is a key technology in advanced semiconductor manufacturing processes.[2] It mainly relies on chemical and mechanical synergy to realize the material's global flattening.[3] With the development of semiconductor process nodes, CMP technology has become more and more important and has become an indispensable planarization process for processes below 0.35 μm.[4] The slurry and pad of the polishing in the CMP system are the main consumables, and the polishing slurry as an active material can significantly affect the polishing performance. Ceria is considered to be the most effective abrasive for polishing SiO_2 substrates due to their unique physical and chemical properties. With the increase in the number and density of multilayer wiring, the circle of CMP process steps has increased significantly, and the impact on the yield of subsequent processes has become greater and greater. Therefore, it is a hot research topic to enhance the polishing efficiency by improving the chemical activity of the abrasive itself rather than increasing the polishing pressure (Higher downforce results in worse surface quality after CMP[5]).

The "chemical tooth" theory proposed by Cook[6] contributed to the study of the polishing mechanism of ceria-based abrasives. The formation and destruction of the Ce–O–Si bond between CeO_2 abrasives and SiO_2 substrate is the key to realizing material removal. The role of Ce^{3+} in CeO_2 abrasives in enhancing this reaction has been widely recognized by researchers. Srinivasan et al.[7] discovered that Ce^{3+} on the surface of CeO_2 abrasives is the key to achieving the removal of SiO_2 materials. Kim et al.[8] studied the polishing performance of CeO_2 abrasives with different specific surface areas and concluded that the small-sized CeO_2 has a higher

☆ **Foundation item:** Project supported by the National Natural Science Foundation of China (51905324), the Scientific Research Program Funded by Shaanxi Provincial Education Department (20JK0545), and the Doctoral Scientific Research Startup Foundation of Shaanxi University of Science and Technology (2018BJ-14).

* Corresponding author. School of Material Science and Engineering, Shaanxi University of Science & Technology, Xi'an, 710021, China.
E-mail address: xuning@sust.edu.cn (N. Xu).

https://doi.org/10.1016/j.jre.2022.10.011
1002-0721/

polishing rate due to the higher Ce^{3+} concentration on the abrasive surface. Therefore, the defects on the ceria surface can enhance the chemical activity of the abrasive, which improves the polishing performance. Doping is a common way to enhance the chemical activity of nanoceria. Younis et al.[9] showed that Gd^{3+} doping enhanced the degradation performance of CeO_2 particles on organic dyes, and the enhanced catalytic activity was attributed to the formation of surface defects on CeO_2 induced by ion doping. Cheng et al.[10] improved the polishing efficiency of CeO_2 abrasives by modifying the surface of commercial particles by ion doping. Furthermore, Kim et al.[11] directly synthesized La^{3+} and Nd^{3+} doped nano-ceria by a traditional hydrothermal method and confirmed the significant effect of doped abrasives on enhancing CMP performance for SiO_2 substrates. These results are attributed to the increased Ce^{3+} concentration on the CeO_2 abrasive surface by ion doping.

In the chip manufacturing process, a fine post-CMP cleaning process is also required to remove the impurity adhesion after CMP.[12] The ion doping can increase the MRR, but post-cleaning of the wafer surface contaminated by impurity ions will become difficult, which will affect the chip quality and even damage the device.[13] Therefore, the preparation of CeO_2 abrasives by controlling atmospheric conditions without introducing impurity ions is an ideal way to increase the Ce^{3+} concentration on the abrasive surface. Choudhury et al.[14] prepared cerium oxide particles with high oxygen vacancy concentration under vacuum conditions, which exhibited better catalytic performance than CeO_2 prepared under air. Lan and Sohn[15] studied cerium oxide prepared under different atmosphere conditions (Air, N_2, H_2), and the results showed that under a reducing atmosphere, cerium oxide has good catalytic performance due to the formation of more oxygen vacancies. However, its wide particle size range and agglomeration behavior cannot be applied in the CMP field. Moreover, the relationship between the oxygen vacancies of CeO_2 surface and Ce^{3+} concentration under the reducing atmosphere has not been deeply studied. To improve the polishing efficiency of conventional CeO_2 abrasives on SiO_2 substrates, the CeO_2 abrasives were prepared by the molten salt method in Air, Ar, and Ar/H_2 atmospheres, respectively, to clarify the influence of CeO_2 abrasives prepared in different atmospheres on the polishing performance of SiO_2 substrate. Through detailed characterization studies, the evolution of crystal structure and micro-morphological of CeO_2 abrasives were analyzed. Although the effect of Ce^{3+} in CeO_2 abrasives on polishing performance has been confirmed, the relationship between the atmospheric environment and the formation of Ce^{3+} on the abrasive surface remains to be further elucidated. In this work, the influence of reducing atmosphere on the concentration of Ce^{3+} on the abrasive surface was emphatically investigated. Moreover, the polishing performance of CeO_2 abrasives prepared in reducing atmosphere and air were compared, and the role of the prepared CeO_2 abrasives on the removal efficiency of SiO_2 substrate was investigated. Finally, the polishing mechanism of the CeO_2 abrasives was discussed through the comprehensive analysis of the morphology, defect characteristics, and polishing performance of the abrasives. To the best of our knowledge, the preparation of CeO_2 abrasives by reducing the atmosphere-assisted molten salt method to enhance the CMP performance on SiO_2 substrates has not been found to be reported yet.

2. Experimental

2.1. Chemical reagents

Cerium nitrate hexahydrate ($Ce(NO_3)_3 \cdot 6H_2O$), potassium chloride (KCl), and sodium chloride (NaCl) are all analytical reagents, and they were all purchased from Sinopharm Chemical Reagent Co., Ltd (China). Analytical reagent ethanol was purchased from Tianjin Fuyu Fine Chemical Co., Ltd. (China). Homemade deionized water was used throughout the experiment. All chemicals were used without further purification. Ar (100% purity) and Ar/H_2 (H_2 concentration of 5%) were used for the experiments.

2.2. Preparation method

The molten salt method was used to prepare CeO_2 powder, and the synthesis steps were as follows. Firstly, the weighed $Ce(NO_3)_3 \cdot 6H_2O$ (2.1711 g), KCl (1.8638 g), and NaCl (1.4610 g) were well ground in an agate mortar. The raw materials in ethanol were mixed completely by magnetic stirring at 300 r/min for 30 min. The mixture was transferred to an alumina crucible and dried in a constant temperature oven at 80 °C to remove absolute ethanol. Then, the OTF-1200X–S tubular atmosphere furnace (Hefei Kejing Material Technology Co., Ltd., China) was used to prepare a mixture containing ceria powder under a certain temperature regime (react at 800 and 700 °C for 2 h, respectively). After cooling down to ambient temperature, the molten salts (KCl–NaCl) in the mixture were washed with hot deionized water to obtain high purity CeO_2 powder. In another experiment, the crucible containing the mixture was heated in the tube furnace with a constant flow (60 mL/min) of Ar or Ar/H_2, respectively, and in the same temperature regime to explore the effect of the surrounding atmosphere. In this work, the abrasives prepared under air, Ar, and Ar/H_2 atmospheres were named CeO_2-Air, CeO_2-Ar, and CeO_2-Ar/H_2, respectively.

2.3. Characterization methods

Powder X-ray diffraction (XRD) patterns of the powders were recorded on a D8 Advance diffractometer (Bruker, Germany) under the condition of Cu Kα radiation range of 20°–120°, and the scanning speed was fixed at 3(°)/min, the Rietveld refinement of powders was characterized using the GSAS program. Fourier transform infrared (FT-IR) spectra were obtained using an FT-IR spectrometer (Bruker, Germany) within the IR range of 500–4000 cm^{-1}. The morphology of the powders was observed with a scanning electron microscope (SEM, Hitachi Regulus 8100, Japan) under secondary electronic mode. Detailed information on morphology and structure was obtained by transmission electron microscopy (TEM, FEI Tecnai G2 F20, USA). Ultraviolet (UV)-visible spectra were recorded with a Cary 5000 UV–Vis–NIR spectrophotometer (Agilent Technologies, USA). X-ray photoelectron spectroscopy (XPS, Thermo Scientific K-Alpha, USA) with Al Kα rays ($h\nu$ = 1486.6 eV) as the excitation source was used for analysis at room temperature, and the binding energy was calibrated with adsorbed carbon (284.8 eV), and the semi-quantitative analysis of the atomic ratio was achieved by measuring the element peak area.

2.4. Polishing experiment

The homemade CeO_2 abrasive was dispersed in deionized water using a ball mill and run at 400 r/min for 5 h. After sufficient dispersion, the slurry was diluted with deionized water to make the solid content 0.5 wt%, and the pH was adjusted to 6.0 with 1 mol/L NaOH solution. The slurry was stirred well by using a magnetic stirrer before the start of the CMP experiment. The quartz glass with the nominal specifications of 20 mm diameter and 2 mm thickness was purchased from Lianyungang Xiongtai Quartz Technology Co., Ltd. A UNIPOL-1200S automatic pressure grinding and polishing machine (Shenyang Kejing Auto-instrument, Co., Ltd., China) equipped with a synthetic leather polishing pad (Shenyang

Kejing Auto-instrument, Co., Ltd., China) was used for CMP experiments. The polishing parameters were set as follows: the platform speed was 80 r/min, the reverse speed of the polishing head was 80 r/min, the pressure applied by the head was 3.5 kg, and the polishing time was 3 min, and the slurry supply rate was 50 mL/min.

The polished quartz glass was cleaned repeatedly in deionized water by ultrasonic and dried for characterization of CMP performance. Surface morphology and roughness were examined by using an atomic force microscope (AFM, Seiko SPA400-SP13800N, Japan) equipped with a silicon nitride tip in contact mode at a scan rate of 1.0 Hz over a scan area of 5 μm × 5 μm. The weight of the workpiece was measured using a precision electronic balance with an accuracy of 0.1 mg. The polishing efficiency or material removal rate (MRR, nm/min) was calculated by the following Eq. (1).[16]:

$$\mathrm{MRR} = \frac{m_0 - m}{\rho \times S \times t} \quad (1)$$

where m_0 and m are the mass of the workpiece before and after polishing, respectively, ρ is the density of the commercial quartz glass used (2.2 g/cm^3), S the area of the workpiece ($\pi \cdot$cm^2), and t the polishing time (3 min). In this experiment, the MRR and roughness data presented are the average of three experiments performed repeatedly.

3. Results and discussion

3.1. Morphology and structure characterization of CeO_2 abrasives

The XRD patterns of the prepared CeO_2 particles are recorded in Fig. 1. All diffraction peaks of the samples match well with the CeO_2 phase of face-centered cubic (fcc) fluorite (JCPDS 34–0394), and no other cerium oxides (Ce_2O_3 species) are found. The peak position analysis of each diffraction spectrum showed that the crystal structure of CeO_2 prepared under different atmospheres changed. The magnification of the diffraction peaks shows that the diffraction peak positions of the samples synthesized under Ar and Ar/H_2 atmospheres are shifted to a higher angle, which may be due to the lattice contraction caused by more oxygen vacancies. The Rietveld refinement of CeO_2 samples was characterized using the GSAS program to further confirm subtle changes in the structure of CeO_2 particles, as shown in Figs. S1(a–c). The Rietveld refinement was attempted using a CeO_2 phase with a face-centered cubic (*Fm*-3*m*) structure. The red circle, the black line, and the blue line represent the recorded, calculated and different profiles for the CeO_2 powder, respectively. For all samples, the refinement parameters (R_p < 7%, R_{wp} < 9%, and Chi^2 < 2) are within a accepted range, indicating that the results of refinement are credible. The results show that the lattice constants and volume of CeO_2-Ar (0.54132 nm, 0.15862 nm^3) and CeO_2-Ar/H_2 (0.54130 nm, 0.15860 nm^3) are smaller than CeO_2-Air (0.54137 nm, 0.15867 nm^3). This further confirms the formation of oxygen vacancies in the CeO_2 crystal. The oxygen vacancies promote the conversion of Ce^{4+} to Ce^{3+} for unit cell charge balance,[17] which is responsible for the increase in Ce^{3+} concentration in CeO_2.[18,19]

The FT-IR spectra of the abrasives are shown in Fig. 2. The spectra were studied to characterize changes in chemical bonds and molecular vibrations, and evaluate the formation of the abrasives. The broad absorption band at 3456 cm^{-1} is due to the presence of the H–O–H stretching mode attributed to the adsorbed water on the CeO_2 abrasive surface.[20–22] The bands at 2927 and 2855 cm^{-1} indicate the C–H stretching mode of the methylene groups,[21,23] and the peak intensity is weakened after synthesis by reducing atmosphere, which indicates that the adsorption of CO_2 by CeO_2 particles is reduced. The bands located at 2160 and 2028 cm^{-1} are due to the stretching vibration of C–H, and CH_2 groups, associated with some of the organic moieties which get physically adsorbed on the surface during sample preparation and handling.[21] The peaks between 1047 and 1630 cm^{-1} correspond to the Ce–O stretching vibrations attributed to the hydrogenated CeO_2 sample.[20,21] The enhancement of the vibrational peak with the reducing atmosphere indicates that the sensitivity of CeO_2 abrasives to hydroxyl groups is elevated, which favors the adsorption of abrasives to SiO_2 substrates. Meanwhile, the existence of the peak at 716 cm^{-1} in the IR spectra is attributed to the asymmetric stretching vibrations between O–Ce–O atoms.[23,24] Furthermore, it verifies the bonding of metal–oxygen existing in the CeO_2 lattice, which is consistent with the XRD results.

Fig. 3 shows the SEM images of the CeO_2 abrasives synthesized under different atmospheres. There are significant differences in the morphology of the particles. From Fig. 3(a–c), it can be seen that the CeO_2-Air, CeO_2-Ar, and CeO_2-Ar/H_2 abrasives are spherical, polyhedral, and octahedral, respectively. Fig. 3(d) shows the schematic diagram of the effect of the atmosphere on the morphology of the abrasives. It is considered that the morphology of CeO_2 particles is gradually transformed from spherical to octahedral with the enhancement of the reducing atmosphere. The morphology of CeO_2 abrasives is one of the factors affecting the CMP performance, and the detailed mechanism of the change of morphology of CeO_2 particles during the synthesis will be focused on in our next study. SEM images also show that all abrasives are in the size range of 200–300 nm, which weakens the influence of abrasive size effect on CMP results.

The TEM images were acquired to further observe the morphology and structure of CeO_2 abrasives. Obviously, with the enhancement of reducibility, the morphology of CeO_2 particles changes significantly. As indicated by the red marks in Figs. S2(a–c), the morphologies of CeO_2 particles are spherical,

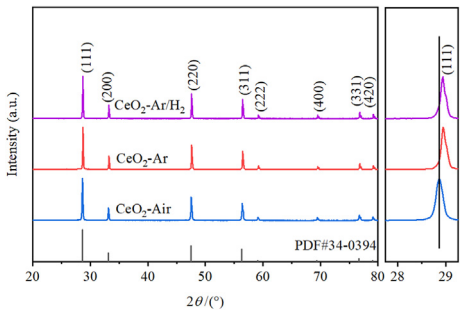

Fig. 1. XRD patterns of the CeO_2 abrasives prepared under the different atmospheres (Air, Ar, Ar/H_2).

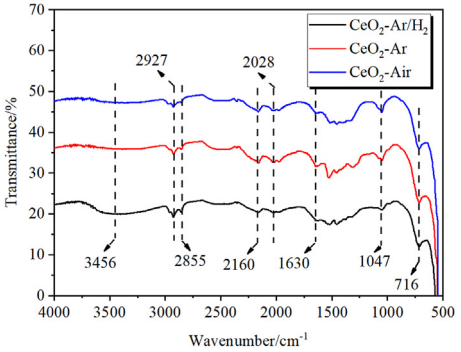

Fig. 2. FT-IR spectra of CeO_2 abrasives prepared under the different atmospheres (Air, Ar, Ar/H_2).

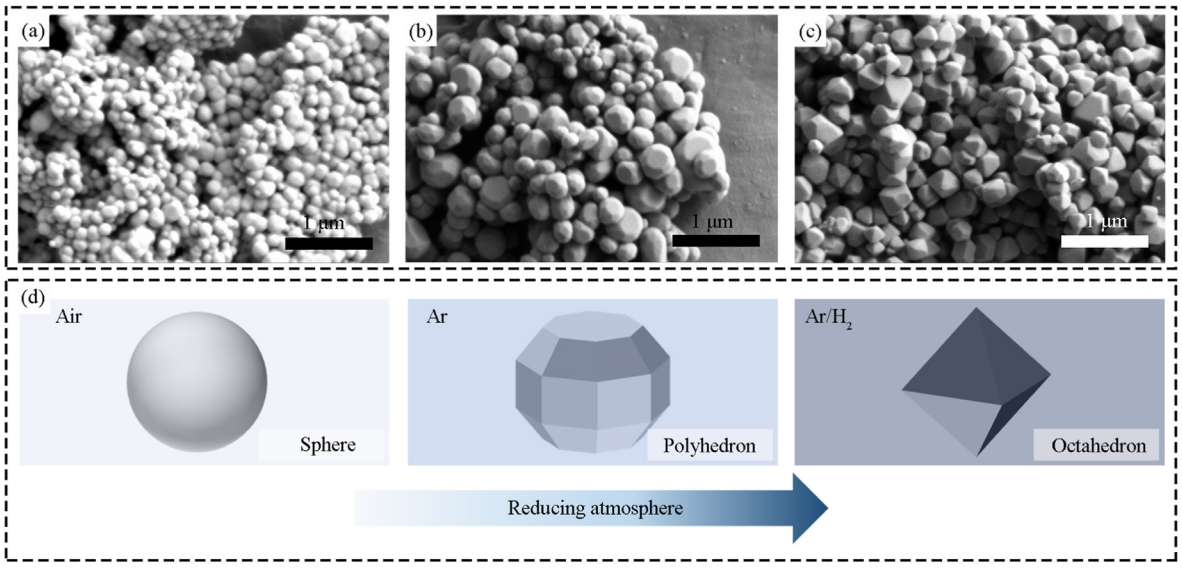

Fig. 3. SEM images of CeO_2 abrasives: (a) CeO_2-Air abrasives; (b) CeO_2-Ar abrasives; (c) CeO_2-Ar/H_2 abrasives; (d) Schematic diagram of the change of abrasive morphology.

polyhedral, and octahedral in order, which is consistent with the SEM results. As shown in Figs. S2(d–f), the boundaries of CeO_2 particles can be observed in the high-resolution TEM (HRTEM) images, and the clear lattice fringe spacing of CeO_2-Air, CeO_2-Ar, and CeO_2-Ar/H_2 particles are 0.318, 0.304 and 0.302 nm, respectively, which correspond to the CeO_2 (111) plane. The results show that the spacing of CeO_2 particles is slightly reduced with the enhancement of the reducibility of the atmosphere. This is attributed to the lattice contraction caused by the generation of oxygen vacancies.

UV–Vis spectroscopy techniques can be used to obtain information on the oxidation state of metal oxide species. The information about the valence state of the Ce element in the prepared CeO_2 samples was preliminarily analyzed by UV–Vis spectroscopy.[25] It is considered that the absorption peak of CeO_2 at 260 nm is attributed to Ce^{3+}, and the absorption peak at 330 nm is attributed to Ce^{4+}.[26,27] Fig. 4 shows the UV–Vis spectra of the as-prepared abrasives, CeO_2-Ar and CeO_2-Ar/H_2 abrasives have high peak intensities, indicating that CeO_2 abrasives prepared under a reducing atmosphere can increase the Ce^{3+} concentration. The CeO_2-Ar and CeO_2-Ar/H_2 abrasives have similar Ce^{3+} concentrations.

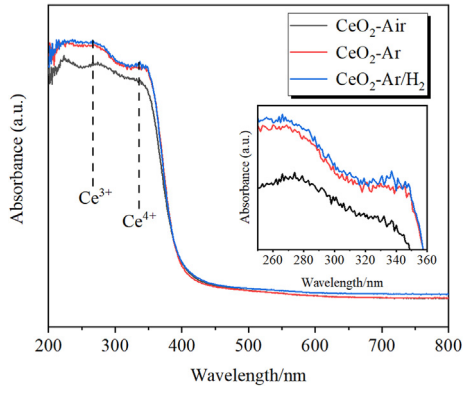

Fig. 4. UV–vis absorption spectra of CeO_2 abrasives prepared under the different atmospheres (Air, Ar, Ar/H_2).

XPS is an analytical technique that detects the composition, chemical state, and concentration of elements on the material surface. The surface chemical composition and valence states of the CeO_2 samples were analyzed by XPS spectroscopy. Fig. 5(a) shows the XPS survey spectra of the particles. The spectra show that only Ce, O, and C elements are detected, and no Cl, Na, or K elements are present in the samples, which also indicates the synthesis of CeO_2 as a single phase. Numerous studies[28–32] have shown that the chemical activity of CeO_2 material is closely related to the concentrations of oxygen vacancy and Ce^{3+}. Therefore, the fine spectra of Ce 3d and O 1s were analyzed in detail by fitting. The spin–orbit splitting energies of the samples are 18.44, 18.44, and 18.30 eV, respectively, which are consistent with the reports.[33] The *u* and *v* are usually used to label the spin orbitals $3d_{3/2}$ and $3d_{5/2}$, where the v_0, *v*', *u*, and *u*' peaks are characteristic peaks of Ce^{3+} and the *v*, *v*'', *v*''', u_0, *u*'', and *u*''' peaks belong to Ce^{4+}.[33,34] As shown in Figs. S3(a–c), the nonlinear peak fitting method was used to identify the peaks of Ce^{3+} and Ce^{4+}, indicating the presence of both Ce^{3+} and Ce^{4+} states in the samples. Table 1 shows the binding energies and peak areas of CeO_2 samples (Air, Ar, Ar/H_2) representing different Ce states. Using the semi-quantitative analysis of the integrated peak area, the Ce^{3+} concentration could be calculated according to Eq. (2).[34] Fig. 5(b) shows the statistics of Ce^{3+} concentration on the CeO_2 abrasive surface. In this work, the Ce^{3+} concentrations on the surface of CeO_2-Air, CeO_2-Ar, and CeO_2-Ar/H_2 abrasives were 23.03 at%, 29.58 at%, and 33.88 at%, respectively. The improvement of Ce^{3+} concentration on the abrasive surface increases with the enhancement of the reducing atmosphere, which was consistent with the UV–Vis results. And this change indicates that there is a state transition between Ce^{4+} to Ce^{3+}, which is excellent for enhanced polishing efficiency.

$$\frac{Ce^{3+}}{Ce^{3+}+Ce^{4+}}=\frac{\text{Area}(v_0,u_0,v',u')}{\text{Total area}} \quad (2)$$

Figs. S3(d–f) display the XPS spectra of O 1s, which can be fitted to three peaks. The peak named O1 can be attributed to lattice oxygen, and the binding energies of this peak for CeO_2 samples prepared under different atmospheres are 529.43 eV (Air), 529.02 eV (Ar), 528.94 eV (Ar/H_2), respectively. The peaks (O2) with binding energies of 531.52 eV (Air), 531.49 eV (Ar) and 531.36 eV

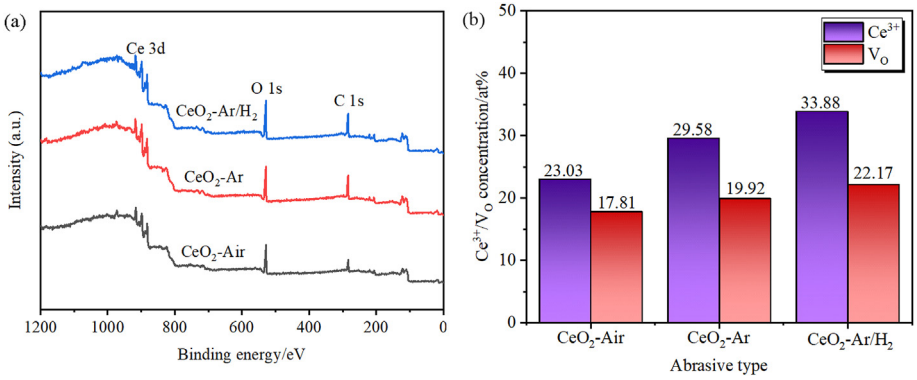

Fig. 5. (a) XPS survey spectra; (b) The concentration of Ce^{3+} and oxygen vacancies.

Table 1
Binding energies and peak areas representing different cerium states in CeO_2 (under Air, Ar, Ar/H_2) samples.

	v_0	v	v'	v''	v'''	u	u_0	u'	u''	u'''
CeO_2-air										
BE (eV)	881.35	882.41	884.52	888.79	898.19	898.95	900.83	902.37	907.69	916.60
Area (%)	7.72	16.91	5.84	11.65	17.23	5.44	11.17	4.04	8.06	11.94
CeO_2-Ar										
BE (eV)	881.13	882.13	883.79	888.26	897.83	898.73	900.55	901.85	907.16	916.28
Area (%)	6.73	10.38	12.23	12.37	17.68	4.66	6.80	8.46	8.45	12.24
CeO_2-Ar/H_2										
BE (eV)	881.21	882.10	883.49	888.35	897.70	898.81	900.46	901.32	907.25	916.20
Area (%)	5.32	8.13	14.34	13.11	18.25	3.69	5.63	9.93	8.97	12.64

(Ar/H_2) are due to the adsorbed oxygen at the oxygen vacancy.[35] In addition, the binding energies of the peaks representing weakly bound oxygen or chemisorbed oxygen peaks[36] are 532.23 eV (Air), 532.23 eV (Ar), and 532.04 eV (Ar/H_2), respectively. The peak positions of CeO_2-Ar and CeO_2-Ar/H_2 samples are shifted to relatively low binding energies, indicating that the reducing atmosphere has a significant effect on the chemical environment of oxygen in CeO_2 samples. The concentrations of oxygen vacancy on the abrasive surface can be obtained by calculating the integral ratio of the fitted peak areas, which are 19.92 at% and 22.17 at% for CeO_2-Ar and CeO_2-Ar/H_2 surfaces, much higher than CeO_2-Air (17.81 at%). It confirms that the preparation of CeO_2 abrasives under a reducing atmosphere can effectively reduce the lattice oxygen and improve the oxygen defects on its surface.

In a reducing atmosphere, the lattice oxygen is spilled out as neutral O_2 molecules and oxygen vacancies are generated in the CeO_2 lattice. The electrons released by the overflow of O_2 molecules are bound around the oxygen vacancy. To keep the crystal electrically neutral, Ce^{4+} in the CeO_2 crystal gains electrons and turns into the lower valence Ce^{3+}, the reaction of defect formation is shown in Eq. (3). As a result, more oxygen vacancies and Ce^{3+} were formed on the surface of CeO_2-Ar and CeO_2-Ar/H_2 abrasives compared to CeO_2-Air abrasives, which facilitated the polishing activity of CeO_2-based abrasives.

$$2Ce_{Ce} + 4O_O = 2Ce'_{Ce} + V_{\ddot{O}} + 3O_O + \frac{1}{2}O_2\uparrow \quad (3)$$

3.2. The polishing performance of CeO_2 abrasives

3.2.1. Material removal rate (MRR) of CeO_2 abrasives on SiO_2 substrates

MRR is one of the important indicators to evaluate the polishing performance of abrasives. Fig. 6 illustrates the MRR of CeO_2 abrasives on SiO_2 substrates, the MRR of CeO_2-Air abrasives is the lowest at 337.60 nm/min, the MRR of CeO_2-Ar abrasives is higher at 578.74 nm/min, and the MRR of CeO_2-Ar/H_2 abrasives is the highest at 691.28 nm/min under the same working conditions. The MRR of CeO_2-Ar and CeO_2-Ar/H_2 abrasives increased by 71.43% and 104.76%, respectively, compared with CeO_2-Air abrasives. These results reveal that the abrasives synthesized under a reducing atmosphere have excellent polishing efficiency. In this work, the Ce^{3+} concentration and morphology of the CeO_2 abrasives synthesized under different atmospheres showed a large variation. The trend of Ce^{3+} concentration is consistent with the improved MRR of abrasives. It is generally accepted that the flattening of rough surfaces involves chemical bonding and mechanical wear between the abrasives and the surface in CMP. Seo et al.[29] believed that the Ce^{3+} concentration could improve the chemical adsorption capacity between the abrasives and the surface. Kim et al.[37] believed that physical morphology is an important factor in enhancing polishing behavior. Therefore, the significant enhancement of polishing efficiency of CeO_2-Ar and CeO_2-Ar/H_2 abrasives is attributed to the increase of Ce^{3+} concentration on the surface of the abrasives synthesized under the reducing atmosphere. Furthermore, the

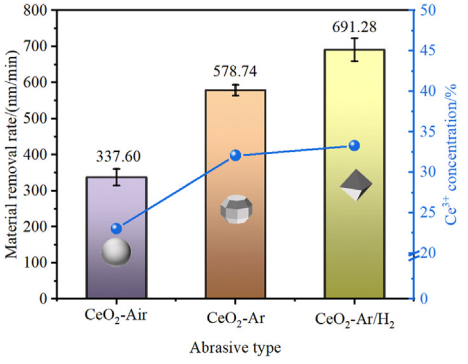

Fig. 6. The results of the evaluation for material removal rate of the CeO_2 abrasives on SiO_2 substrates.

MRR of CeO_2-Ar/H_2 abrasives is improved by 19.45% compared with CeO_2-Ar abrasives, which may be attributed to the octahedral morphology that enhances mechanical interaction during CMP. In addition, we collected the values of MRR for different types of CeO_2-based abrasives in some works, as shown in Fig. S4. For the core/shell abrasives, the present results show a poor MRR, although the structure of the abrasive has been designed and regulated to improve CMP performance, it is still far from being suitable for large-scale commercial use. For the doped abrasives, it is believed that the doping increases the Ce^{3+} concentration on the abrasive surface, which enhances the MRR. However, impurity ions of the abrasives during the polishing will pollute the surface of the substrate leading to difficulties in CMP cleaning, and residual impurity ions will negatively affect or even damage the device. Under the existing studies and applications, it is very feasible to enhance MRR by adjusting the physical properties (size and morphology) of pure CeO_2 abrasive, but the improvement of the approach is limited. In this work, the pure CeO_2 abrasives synthesized under a reducing atmosphere not only changed the morphology but also improved the chemical activity of the CeO_2 abrasives, which together improved the removal efficiency.

3.2.2. *Surface quality of SiO_2 substrates after CMP*

To confirm the effect of material surface quality after polishing with homemade abrasives. As shown in Fig. 7, the surface morphology of the quartz glass was characterized using AFM. The two-dimensional surface morphology of quartz glass before and after polishing are shown in Fig. 7(a–d). The light and dark colors in the graph show the surface roughness, where dark areas indicate the valleys and light areas indicate the peaks. Concretely, the roughness average (R_a) and the root mean square roughness (R_q) of the surface are shown in Fig. 7(f). The initial roughness of quartz glass is 0.955 nm, and all of them are improved (0.391, 0.537, and 0.521 nm) after polishing with the CeO_2 slurry, in which the polishing slurry formulated with CeO_2-Ar and CeO_2-Ar/H_2 abrasives synthesized under reducing atmosphere has poorer polishing performance in surface quality. The difference in surface quality after polishing may be caused by the different morphology of abrasives. The sharped morphology reduced contact areas between abrasives and surfaces, which leads to enhanced contact stress reducing the surface quality.[38] As shown in Fig. 7(e), the profile roughness in the selected area (the diagonal in Fig. 7(a–d)) was also analyzed, where the *Z*-axis represents the depth of the line profile, and the *X*-axis represents the length. The improved surface planarization degree can be confirmed by reduced topographical variations. Moreover, compared with the initial surface, rough peaks or valleys are evenly distributed on the polished surface, which is conducive to the improvement of the overall surface quality.

3.3. *CMP mechanism of CeO_2 abrasives prepared under reducing atmosphere*

In this work, CeO_2 abrasives were prepared under the reducing atmosphere. The surface quality of the SiO_2 substrate was significantly improved after polishing with the abrasives. In particular, the abrasives have excellent polishing efficiency, which is attributed to a combination of the following factors. The analysis of the structure and chemical valence of the as-prepared CeO_2 particles showed that the surface of the abrasive has a higher Ce^{3+} concentration. The CMP performance also confirmed that the polishing efficiency of the abrasives with a high Ce^{3+} concentration is significantly improved. There may be a positive function between the Ce^{3+} concentration and MRR, which may be due to the electron transfer of Ce^{3+} promoting Ce–O–Si bond breaking. Furthermore, the polishing results also show that the MRR of the CeO_2-Ar/H_2 abrasives is 19.45% higher than that of the CeO_2-Ar abrasives even when the chemical activity (Ce^{3+} concentration) is similar, which may be attributed to the effect of abrasive morphology.

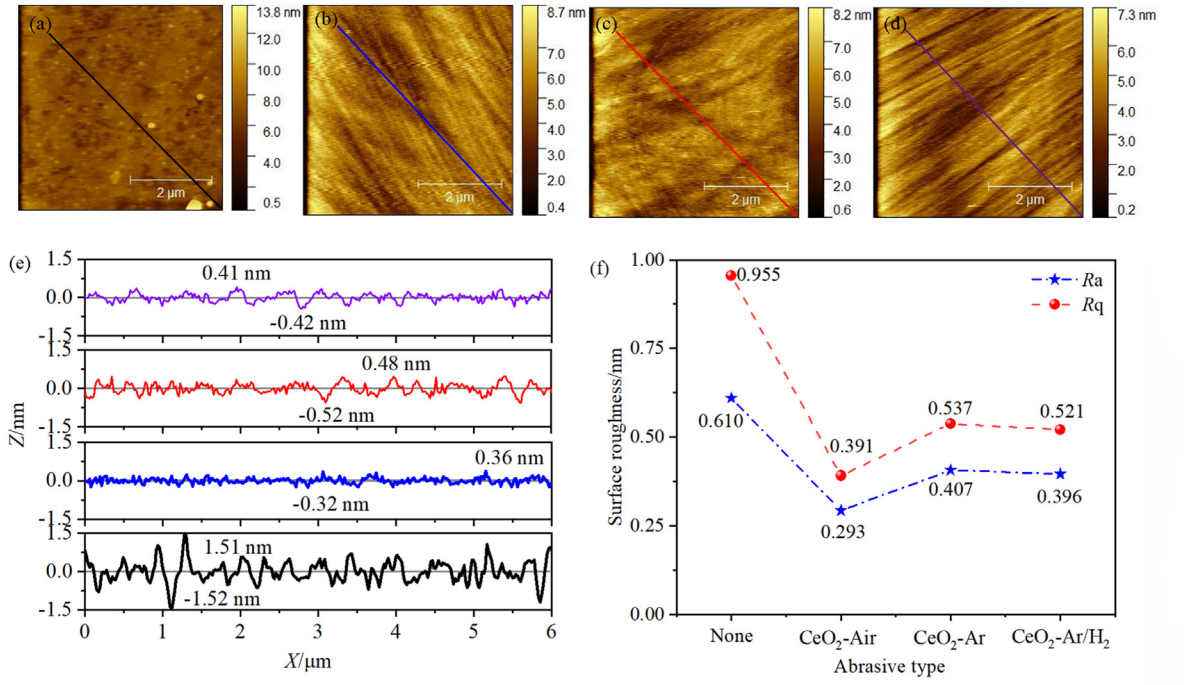

Fig. 7. AFM images of the substrate surface after CMP: 2D images after CMP without abrasives (a) and with CeO_2-Air abrasives (b), CeO_2-Ar abrasives (c), CeO_2-Ar/H_2 abrasives (d); (e) The corresponding profile line curve; (f) The results of the evaluation for surface roughness.

Fig. 8 is a schematic diagram of the polishing mechanism of CeO_2 abrasives prepared under different atmospheres on the SiO_2 substrate. The synergy of chemistry and mechanics in the CMP process is what makes the material surface flat. The CeO_2 abrasives not only have moderate mechanical properties but also provide chemical activity in the CMP process. As shown in Fig. 8(a), the CeO_2 abrasives with nearly spherical morphology were prepared under air, and the contact stress is small under the downforce, which only removes the superficial atoms on the surface. The spherical particles may have both sliding and rolling removal behaviors on SiO_2 substrates. The sliding friction behavior of abrasives is considered to be the main mode of material removal, while the rolling behavior of some abrasives weakens the material removal ability due to reduced friction. As shown in Fig. 8(b), the CeO_2 abrasives with octahedral morphology were prepared under a reducing atmosphere. Its sharp edges enable the abrasives to have stronger compressive stress at the contact surface. On the one hand, it increases the material removal from the deeper layers of the substrate by the abrasives during the CMP, and on the other hand, the enhanced mechanical action further promotes the chemical reaction at the interface. As shown in Fig. S5, the stress distribution on the surface of the SiO_2 substrate when the spherical and octahedral abrasives were indented at a depth of 50 nm was simulated by finite element analysis (FEA), respectively. The abrasives with octahedral morphology achieved the same indentation depth as spherical particles under lower compressive stress, which verifies that the abrasives with octahedral morphology have a higher MRR. The chemical activity of the CeO_2 abrasives is an advantage that distinguishes it from other abrasives, which significantly enhances the CMP performance of the abrasives. As shown in Fig. 8(c), the CeO_2 abrasives reacted with the SiO_2 substrate to form Ce–O–Si bonds in the slurry, the offset of the electron cloud strengthens the Ce–O–Si bonds and weakens the Si–O–Si bonds, then the surface layer of the substrate is removed by abrasives under the mechanical force. As shown in Fig. 8(d), Ce^{4+} on the surface of the CeO_2 abrasives is reduced to Ce^{3+} with higher reactivity under the reducing atmosphere. After the Ce–O–Si bond is formed between the abrasives and the substrate surface, the free electrons in Ce^{3+} break the Si–O–Si bond through electron transfer, which significantly increases the material removal efficiency.

In the CMP, the hydrated surface layer ($Si(OH)_4$) is removed by the tribochemical reaction or/and mechanical force of the

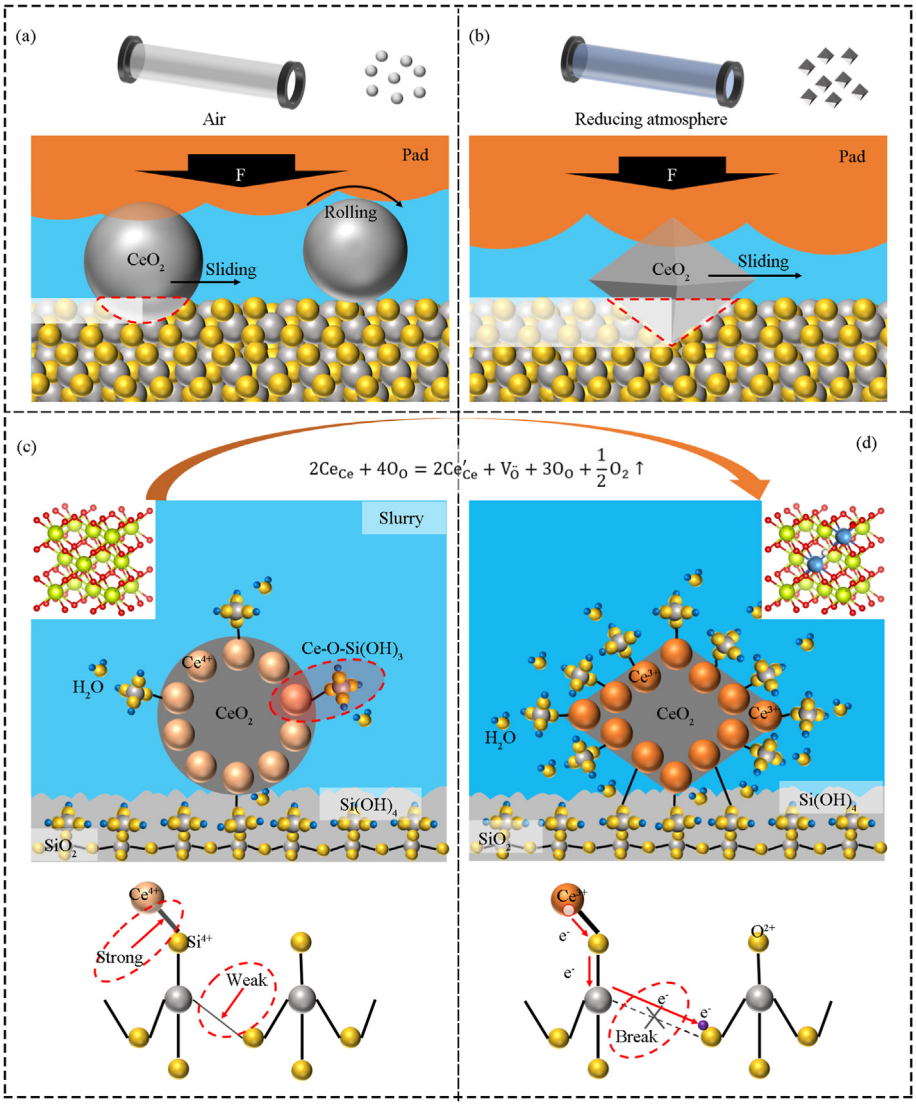

Fig. 8. Schematic diagram of the polishing mechanism of CeO_2 abrasives prepared under different atmospheres on SiO_2 substrate: (a, c) Air; (b, d) Reducing atmosphere.

abrasives.[39] The material removal is closely related to the frictional effect of the two/three-body contact at the interface. In previous work,[40,41] we indirectly used the CeO_2 tip to study its frictional behavior. It is believed that studying the friction behavior of abrasives with different properties at the interface is the key to quantitatively analyzing the relationship between abrasives and MRR. In the next work, we will study the CMP behavior of CeO_2 abrasives under multi-factors through a series of experiments and FEA.

4. Conclusions

CeO_2-Air, CeO_2-Ar, and CeO_2-Ar/H_2 abrasives with different surface defect concentrations were prepared by reducing atmosphere-assisted molten salt method, which were used for CMP of SiO_2 substrates. XRD and Rietveld refinement confirm that the CeO_2 lattice shrinks due to the formation of oxygen vacancies with the enhancement of the reducing atmosphere. SEM images observe that the morphology of the abrasive prepared under a reducing atmosphere gradually changes from spherical to octahedral. The analysis of XPS patterns confirms the higher concentration of defects on the surface of the abrasives prepared under a reducing atmosphere. CMP experiments on SiO_2 substrates indicate that the prepared abrasives all significantly improve the surface quality. Obviously, CeO_2-Ar and CeO_2-Ar/H_2 abrasives have very strong polishing efficiency (578.74 and 691.28 nm/min), with MRR increases of 71.43% and 104.76%, respectively, compared to CeO_2-Air abrasives. The enhanced polishing efficiency can be attributed to the elevated chemical activity (Ce^{3+} concentration) of the CeO_2 abrasives prepared under the reducing atmosphere, which enhances the chemisorption and bonding between the CeO_2 abrasives and the SiO_2 surface. The morphology of the abrasives further affects the MRR, where the sharp edges of the abrasives enhance the frictional behavior of the interface, thereby accelerating material removal. In this work, the CeO_2 abrasive prepared in a reducing atmosphere has the advantages of high-speed polishing and improved surface quality, which can significantly improve the CMP performance.

Declaration of competing interest

The authors declare that they have no conflict of interest.

Appendix A. Supplementary data

Supplementary data to this article can be found online at https://doi.org/10.1016/j.jre.2022.10.011.

References

1. Wang WT, Zhang BG, Shi YH, Zhou JK, Wang R, Zeng NY. Improved chemical mechanical polishing performance in 4H-SiC substrate by combining novel mixed abrasive slurry and photocatalytic effect. *Appl Surf Sci*. 2022;575:151676.
2. Janoš P, Ederer J, Pilařová V, Henych J, Tolasz J, Milde D, et al. Chemical mechanical glass polishing with cerium oxide: effect of selected physico-chemical characteristics on polishing efficiency. *Wear*. 2016;362–363:114.
3. Chen AL, Wang TY, Chen Y, Wang SR, Chen Y. Development of polystyrene/polyaniline/ceria (PS/PANI/CeO_2) multi-component abrasives for photochemical mechanical polishing/planarization applications. *Appl Surf Sci*. 2022;575:151784.
4. Krishnan M, Nalaskowski JW, Cook LM. Chemical mechanical planarization: slurry chemistry, materials, and mechanisms. *Chem Rev*. 2010;110:178.
5. Xiao C, Chen C, Guo J, Zhang P, Chen L, Qian LM. Threshold contact pressure for the material removal on monocrystalline silicon by SiO_2 microsphere. *Wear*. 2017;376–377:188.
6. Cook LM. Chemical processes in glass polishing. *J Non-Cryst Solids*. 1990;120(1–3):152.
7. Srinivasan R, Dandu PVR, Babu SV. Shallow trench isolation chemical mechanical planarization: a review. *ECS J. Solid State Sci. Technol.* 2015;4(11):P5029.
8. Kim K, Yi DK, Paik U. Increase in Ce^{3+} concentration of ceria nanoparticles for high removal rate of SiO_2 in chemical mechanical planarization. *ECS J. Solid State Sci. Technol.* 2017;6(9):P681.
9. Younis A, Shirsath SE, Shabbir B, Li S. Controllable dynamics of oxygen vacancies through extrinsic doping for superior catalytic activities. *Nanoscale*. 2018;10(39):18576.
10. Cheng J, Huang S, Li Y, Wang TQ, Xie L, Lu XC. RE (La, Nd and Yb) doped CeO_2 abrasive particles for chemical mechanical polishing of dielectric materials: experimental and computational analysis. *Appl Surf Sci*. 2020;506:144668.
11. Kim E, Lee J, Bae C, Seok H, Kim H-U, Kim T. Effects of trivalent lanthanide (La and Nd) doped ceria abrasives on chemical mechanical polishing. *Powder Technol*. 2022;397:117025.
12. Ng D, Huang PY, Jeng YR, Liang H. Nanoparticle removal mechanisms during post-CMP cleaning. *Electrochem Solid State Lett*. 2007;10(8):H227.
13. Zhang JH, Huang H, Greene AM, Xie R, Seo S-C, Montanini P, et al. CMP challenges for advanced technology nodes. *MRS Adv*. 2017;2(44):2361.
14. Choudhury B, Chetri P, Choudhury A. Oxygen defects and formation of Ce^{3+} affecting the photocatalytic performance of CeO_2 nanoparticles. *RSC Adv*. 2014;4(9):4663.
15. Lan Y-P, Sohn HY. Nanoceria synthesis in molten KOH-NaOH mixture: characterization and oxygen vacancy formation. *Ceram Int*. 2018;44(4):3847.
16. Zhang ZY, Liu J, Hu W, Zhang LZ, Xie WX, Liao LX. Chemical mechanical polishing for sapphire wafers using a developed slurry. *J. Manuf. Mater. Process.* 2021;62:762.
17. Chen DK, He DD, Lu JC, Zhong LP, Liu F, Liu JP, et al. Investigation of the role of surface lattice oxygen and bulk lattice oxygen migration of cerium-based oxygen carriers: XPS and designed H_2-TPR characterization. *Appl Catal, B*. 2017;218:249.
18. Dutta P, Pal S, Seehra MS, Shi Y, Eyring EM, Ernst RD. Concentration of Ce^{3+} and oxygen vacancies in cerium oxide nanoparticles. *Chem Mater*. 2006;18(21):5144.
19. Agarwal S, Zhu X, Hensen EJM, Mojet BL, Lefferts L. Surface-dependence of defect chemistry of nanostructured ceria. *J Phys Chem C*. 2015;119(22):12423.
20. Majeed Khan MA, Khan W, Naziruddin Khan M, Alhazaa AN. Enhanced visible light-driven photocatalytic performance of Zr doped CeO_2 nanoparticles. *J Mater Sci Mater Electron*. 2019;30(9):8291.
21. Khakhal HR, Kumar S, Dolia SN, Dalela B, Vats VS, Hashmi SZ, et al. Oxygen vacancies and F^+ centre tailored room temperature ferromagnetic properties of CeO_2 nanoparticles with Pr doping concentrations and annealing in hydrogen environment. *J Alloys Compd*. 2020;844:156079.
22. Wang L, Xu GY, Liu CY, Hou HL, Tan SJ. Surface-modified CeO_2 coating with excellent thermal shock resistance performance and low infrared emissivity at high-temperature. *Surf Coat Technol*. 2019;357:559.
23. Junais PM, Athika M, Govindaraj G, Elumalai P. Supercapattery performances of nanostructured cerium oxide synthesized using polymer soft-template. *J Energy Storage*. 2020;28:101241.
24. Subramanyam K, Sreelekha N, Reddy DA, Ramanathan M, Poornaprakash B, Reddy KC, et al. Influence of transition metals co-doping on CeO_2 magnetic and photocatalytic activities. *Ceram Int*. 2020;46(4):5086.
25. Singh R, Singh S. Role of phosphate on stability and catalase mimetic activity of cerium oxide nanoparticles. *Colloids Surf, A*. 2015;132:78.
26. Kim E, Hong J, Hong S, Kanade C, Seok H, Kim H-U, et al. Improvement of oxide removal rate in chemical mechanical polishing by forming oxygen vacancy in ceria abrasives via ultraviolet irradiation. *Mater Chem Phys*. 2021;273:124967.
27. Yang YS, Mao Z, Huang WJ, Liu LH, Li JL, Li JL, et al. Redox enzyme-mimicking activities of CeO_2 nanostructures: intrinsic influence of exposed facets. *Sci Rep*. 2016;6:35344.
28. Matussin SN, Harunsani MH, Khan MM. CeO_2 and CeO_2-based nanomaterials for photocatalytic, antioxidant and antimicrobial activities. *J Rare Earths*. 2023;41(2):167.
29. Seo J, Moon J, Kim JH, Lee K, Hwang J, Yoon H, et al. Role of the oxidation state of cerium on the ceria surfaces for silicate adsorption. *Appl Surf Sci*. 2016;389:311.
30. Xia XW, Lan YP, Li JQ, Chen CY, Xu BJ, Luo X, et al. Facile synthesis of nanoceria by a molten hydroxide method and its photocatalytic properties. *J Rare Earths*. 2020;38(9):951.
31. Zhang Y-C, Li Z, Zhang L, Pan L, Zhang X, Wang L, et al. Role of oxygen vacancies in photocatalytic water oxidation on ceria oxide: experiment and DFT studies. *Appl Catal, B*. 2018;224:101.
32. Bao TT, Zhou H, Zhang Y, Guo CX, Guo WM, Qin H, et al. Effect of CeO2 on carbon deposition resistance of Ni/CeO2 catalyst supported on SiC porous ceramic for ethanol steam reforming. *J Rare Earths*. 2022. https://doi.org/10.1016/j.jre.2022.09.006. In press.
33. Soni S, Vats VS, Kumar S, Dalela B, Mishra M, Meena RS, et al. Structural, optical and magnetic properties of Fe-doped CeO_2 samples probed using X-ray photoelectron spectroscopy. *J Mater Sci Mater Electron*. 2018;29(12):10141.
34. Chen AL, Duan YH, Mu ZY, Cai WJ, Chen Y. Meso-silica/Erbium-doped ceria binary particles as functionalized abrasives for photochemical mechanical polishing (PCMP). *Appl Surf Sci*. 2021;550:149353.
35. Pan J, Wang SR, Chen AL, Chen Y, Wang MH, Chen Y. Visible-light-active mesoporous ceria (CeO_2) nanospheres for improved photocatalytic performance. *J Alloys Compd*. 2022;898:162895.
36. Liu X, Ding J, Lin X, Gao RH, Li ZH, Dai W-L. Zr-doped CeO_2 nanorods as versatile catalyst in the epoxidation of styrene with tert-butyl hydroperoxide as the oxidant. *Appl Catal, A*. 2015;503:117.

37. Kim YH, Jung YG, Yoon GS, Moon J, Watanabe A, Naito M, et al. Non-Prestonian behavior of rectangular shaped ceria slurry in shallow trench isolation chemical mechanical planarization. *J Nanosci Nanotechnol*. 2012;12(3):2810.
38. Hu PF, Chen Y, Sun R, Chen Y, Yin YR, Wang ZC. Synthesis, characterization and frictional wear behavior of ceria hybrid architectures with {111} exposure planes. *Appl Surf Sci*. 2017;401:100.
39. Hoshino T, Kurata Y, Terasaki Y, Susa K. Mechanism of polishing of SiO_2 films by CeO_2 particles. *J Non-Cryst Solids*. 2001;283:129.
40. Xu N, Han WZ, Wang YC, Li J, Shan ZW. Nanoscratching of copper surface by CeO_2. *Acta Mater*. 2017;124:343.
41. Xu N, Ma JH, Liu Q, Han WZ, Shan ZW. Size effect of CeO_2 particle on nanoscale single-asperity sliding friction. *Tribol Lett*. 2022;70(4), 1.